Received: 26 May 2022 | Revised: 11 January 2023 | Accepted: 12 January 2023

DOI: 10.1097/HEP.0000000000000319

ORIGINAL ARTICLE

OPEN

Tyrosine kinase receptor B attenuates liver fibrosis by inhibiting TGF-β/SMAD signaling

Yu Song[1,2] | Jiayi Wei[1,2] | Rong Li[3] | Ruifeng Fu[4] | Pei Han[5] | Heming Wang[1,2] | Guangcong Zhang[1,2] | Shuyu Li[1,2] | Sinuo Chen[1,2] | Zhiyong Liu[1,2] | Yicheng Zhao[6,7] | Changfeng Zhu[1,2] | Jimin Zhu[1,2] | Shuncai Zhang[1,2] | Hao Pei[8] | Jiefei Cheng[5,9] | Jian Wu[1,2,10] | Ling Dong[1,2] | Guangqi Song[1,7] | Xizhong Shen[1,2] | Qunyan Yao[1,2]

[1]Department of Gastroenterology and Hepatology, Zhongshan Hospital, Fudan University, Shanghai, China

[2]Shanghai Institute of Liver Diseases, Shanghai, China

[3]Department of Neurosurgery, Shanghai Changhai Hospital, Naval Medical University, Shanghai, China

[4]Shanghai Key Lab of Cell Engineering, Translational Medicine Research Center, Naval Medical University, Shanghai, China

[5]Otsuka Shanghai Research Institute, Shanghai, China

[6]Key Laboratory of Organ Regeneration and Transplantation of the Ministry of Education, Center for Pathogen Biology and Infectious Diseases, The First Hospital of Jilin University, Changchun, China

[7]Joint Laboratory of Biomaterials and Translational Medicine, Puheng Technology, Suzhou, China

[8]Shanghai Key Laboratory of Green Chemistry and Chemical Processes, School of Chemistry and Molecular Engineering, East China Normal University, Shanghai, China

[9]Shanghai University of Traditional Chinese Medicine, Shanghai, China

[10]MOE/NHC/CAMS Key Laboratory of Medical Molecular Virology, Department of Medical Microbiology and Parasitology, School of Basic Medical Sciences, Fudan University, Shanghai, China

Correspondence
Qunyan Yao, Department of Gastroenterology and Hepatology, Zhongshan Hospital, Shanghai Institute of Liver Diseases, Fudan University, 180 Fenglin Road, Shanghai 200032, China. Email: yao.qunyan@zs-hospital.sh.cn

Xizhong Shen, Department of Gastroenterology and Hepatology, Zhongshan Hospital, Shanghai Institute of Liver Diseases, Fudan University, 180 Fenglin Road, Shanghai 200032, China. Email: shen.xizhong@zs-hospital.sh.cn

Guangqi Song, Department of Gastroenterology and Hepatology, Zhongshan Hospital, Fudan University,180 Fenglin Road, Shanghai, 200032, China. Joint Laboratory of Biomaterials

Abstract

Background and Aims: Liver fibrosis is a leading indicator for increased mortality and long-term comorbidity in NASH. Activation of HSCs and excessive extracellular matrix production are the hallmarks of liver fibrogenesis. Tyrosine kinase receptor (TrkB) is a multifunctional receptor that participates in neurodegenerative disorders. However, paucity of literature is available about TrkB function in liver fibrosis. Herein, the regulatory network and therapeutic potential of TrkB were explored in the progression of hepatic fibrosis.

Abbreviations: 3D, 3-dimensional; AAV6, adeno-associated virus vector serotype 6; AAV8, adeno-associated virus vector serotype 8; BDNF, Brain-derived neurotrophic factor; CDK, cyclin-dependent kinase; CDS, Coding domain sequence; co-IP, coimmunoprecipitation; DEGs, differentially expressed genes; Erk, extracellular regulated kinase; GFP, green fluorescent protein; IP, immunoprecipitation; Ndfip1, Nedd4 family interacting protein-1; PA, palmitic acid; H&E, hematoxylin and eosin; PI3K, phosphatidylinositol-3 kinase; qRT-PCR, quantitative reverse transcriptase PCR; SBEs, SMAD-binding elements; RFP, Red Fluorescent Protein; TrkB, tyrosine kinase receptor B; YFP, yellow fluorescent protein.

Yu Song, Jiayi Wei, Rong Li, and Ruifeng Fu contributed equally.

Supplemental Digital Content is available for this article. Direct URL citations are provided in the HTML and PDF versions of this article on the journal's website, www.hepjournal.com

and Translational Medicine, Puheng Technology, 188 Fuchun Jiang Road, Suzhou, Jiangsu, 215009, China.
Email: guangqi.song@puhengtec.com

Ling Dong, Department of Gastroenterology and Hepatology, Zhongshan Hospital, Shanghai Institute of Liver Diseases, Fudan University, 180 Fenglin Road, Shanghai 200032, China.
Email: dong.ling@zs-hospital.sh.cn

Jian Wu, School of Basic Medical Sciences, Fudan University Shanghai Medical College, 138 Yixue Yuan Road, P.O. Box 228, Shanghai 200032, China.
Email: jian.wu@fudan.edu.cn

Methods and Results: The protein level of TrkB was decreased in mouse models of CDAHFD feeding or carbon tetrachloride-induced hepatic fibrosis. TrkB suppressed TGF-β-stimulated proliferation and activation of HSCs in 3-dimensional liver spheroids and significantly repressed TGF-β/SMAD signaling pathway either in HSCs or in hepatocytes. The cytokine, TGF-β, boosted Nedd4 family interacting protein-1 (Ndfip1) expression, promoting the ubiquitination and degradation of TrkB through E3 ligase Nedd4-2. Moreover, carbon tetrachloride intoxication-induced hepatic fibrosis in mouse models was reduced by adeno-associated virus vector serotype 6 (AAV6)–mediated TrkB overexpression in HSCs. In addition, in murine models of CDAHFD feeding and Gubra-Amylin NASH (GAN), fibrogenesis was reduced by adeno-associated virus vector serotype 8 (AAV8)–mediated TrkB overexpression in hepatocytes.

Conclusion: TGF-β stimulated TrkB degradation through E3 ligase Nedd4-2 in HSCs. TrkB overexpression inhibited the activation of TGF-β/SMAD signaling and alleviated the hepatic fibrosis both *in vitro* and *in vivo*. These findings demonstrate that TrkB could be a significant suppressor of hepatic fibrosis and confer a potential therapeutic target in hepatic fibrosis.

INTRODUCTION

Hepatic fibrosis is characterized as an abnormal wound-healing response elicited by persistent chronic liver injury.[1] On liver injury, activating quiescent HSCs are the dominant driver of fibrogenesis. The deposition of extracellular matrix components secreted by activated HSCs disrupts liver structure.[2] Hepatic fibrosis may progress into cirrhosis and cancer when the etiology cannot be eliminated. No effective medications have been approved yet.[3] Thus, there is an urgency to comprehensively understand the pathogenesis of hepatic fibrosis to identify novel targets to halt fibrotic progression in chronic liver injury.

TGF-β is a well-known profibrotic cytokine. TGF-β secretion increases in the fibrotic microenvironment when an injury occurs and excites SMAD2/3 activation through TGF-β receptor1/2 (TGFBR1/2).[4] Subsequently, the phosphorylated SMAD2/3 was translocated into the nucleus to initiate the expression of extracellular matrix components through directly targeting downstream genes, such as *PAI1*, *CTGF*, and *c-Jun*.[5] Several inhibitors for TGF-β/SMAD signaling were identified to block hepatic fibrosis.[6] However, targeting the ubiquitously expressed TGF-β could be associated with unacceptable adverse consequences.[6] Therefore, organ-specific regulation of TGF-β signaling could be a promising strategy for the intervention of hepatic fibrosis.[7]

Tyrosine kinase receptor (TrkB) is known as a high-affinity receptor for brain-derived neurotrophic factor (BDNF). Many studies have demonstrated that TrkB participates in regulating neuronal differentiation, synapse formation, and neurite branching through activating PI3K/Akt, PLCγ/PKC, and Ras/Erk signaling.[8] Because of the poor druggability of BDNF, TrkB agonists are proposed to be potential therapeutics for neurological disorders.[9] Recently, TrkB agonistic antibody Ab4B19 was demonstrated to successfully reverse premature ovarian failure.[10] On the other hand, the products of TrkB gene fusions are identified as oncogenic drivers in various cancer types.[11] Tyrosine kinase inhibitors, such as entrectinib and laratrectinib, targeting the genetic alterations, have been approved for the treatment of NTRK fusion–positive solid tumors by the Food and Drug Administration.[12] Moreover, it is reported that TrkB is associated with obesity and atherogenesis,[13,14] indicating a potential role of TrkB in lipid metabolism. However, the relevance of TrkB in the progression of chronic liver disease has poorly been understood.

The present study found that abnormal TrkB expression was well correlated with the progression of liver fibrosis. Increased TrkB repressed HSC proliferation and activation *in vitro* by suppressing the phosphorylation of TGF-β–stimulated SMAD2/3. TGF-β1–induced Nedd4 family interacting protein-1 (Ndfip1) promoted the degradation of TrkB through the ubiquitin-proteasome pathway. adeno-associated virus vector serotype 8 (AAV8)–mediated or AVV6-mediated overexpression of TrkB in hepatocytes or HSCs reduced the progression of liver fibrosis in murine models. Taken together, the findings

underscore the novel functions of TrkB in ameliorating the pathogenesis of liver fibrosis and represent its therapeutic potential for liver fibrosis.

METHODS

Animals and treatment

All animal experiments followed procedures approved by the Institutional Animal Care and Use Committee (IACUC) of Zhongshan Hospital, Fudan University. Male C57BL/6J and ob/ob mice aged 6–8 weeks were purchased from JSJ Company (Shanghai, China). Two different NASH mouse models were established. Male mice at 6-week old were fed a CDAHFD (~0.1% methionine, 0% choline) diet with 60 kcal% fat (A06071302, Research Diets, NJ) for 9 weeks. AAV8 vectors were injected through the tail vein in the third and sixth week in a dose of 1×10^{11} vector genomes/g (VG/g). Male ob/ob mice at 8-week old were fed a Gubra-Amylin NASH (GAN) diet (D09100310, Research Diets, NJ) for 16 weeks. AAV8 vectors were injected through the tail vein in the eighth and 12th week in a dose of 1×10^{11} VG/g. Carbon tetrachloride (CCl_4) was used to induce liver fibrosis in mice. Male mice at 8-week old were i.p. injected with CCl_4 at 0.6 μL/g body weight (1:10 v/v in corn oil from Sigma-Aldrich) twice weekly for 8 weeks. Adeno-associated virus vector serotype 6 (AAV6) vectors were injected through the tail vein in the fourth week with a dose of 2×10^{11} VG/g. Mice livers were harvested at the end of each experiment.

Patients and sample collection

A total of 62 specimens of human liver fibrosis were obtained at Zhongshan Hospital, Fudan University. Informed consent was obtained from all participants before enrollment. The study was approved by the Institutional Ethics Committee of Zhongshan Hospital of Fudan University (no. B2021-485) and conducted following the Declaration of Helsinki and Istanbul. All clinical specimens were collected from enrolled patients.

Histological staining

Liver samples were fixed with 4% paraformaldehyde (Sigma-Aldrich) for 20 minutes and stained following a standard protocol. Hematoxylin and eosin and Sirius red staining were conducted on paraffin-embedded liver sections to visualize liver morphology and to assess fibrotic stages. Hepatic fibrosis, as visualized by immunohistochemistry, was photometrically semiquantitated by ImageJ software in a blinded manner. The sources of antibodies used for immunohistochemical staining are listed in Table S1 (http://links.lww.com/HEP/D445).

Cell culture and treatment

Hepatoma HepG2 cells were purchased from the National Collection of Authenticated Cell Cultures (serial no. SCSP-510). Human hepatic stellate LX2 cells were purchased from Millipore (serial no. SCC064). HepG2 and LX2 cells were cultured in DMEM medium with 10% fetal bovine serum in the atmosphere with 5% CO_2 at 37 °C. For TGF-β1 treatment, cells were starved for 24 hours with fetal bovine serum–free DMEM medium overnight and then treated with TGF-β1 at 10 ng/mL (Abcam, ab50036).

3D liver spheroid construction

3D liver spheroids were constructed with HepG2 and LX2 cells in 384-well Corning microplates (Cat. 4516). Both cell types were assembled with DNA Origamis in a ratio of 10:1 (50,000 cells per spheroid). Spheroids were cultured in DMEM medium with 10% fetal bovine serum for 24 hours and used for subsequent treatments.

Co-Immunoprecipitation

LX2 cells were transfected with indicated plasmids for 48 hours and lysed with immunoprecipitation buffer. Then the lysates were incubated with anti-DYKDDDDK (Flag) affinity gel (20585ES03, Yeasen, Shanghai, China) or protein A/G agarose beads (20423, Thermo Scientific) and antibody overnight at 4 °C on rotating wheel. Affinity gel or beads were washed 5 times with cold PBS. Western blotting analysis was performed for protein detection.

TGF-β cell–based assay

HEK-Blue TGF-β cells (InvivoGen, Cat. hkb-tgfb) were used to monitor the activation of the TGF-β/SMAD pathway. TrkB was overexpressed in HEK-Blue TGF-β cells by lentiviral transduction. After TGF-β1 treatment for 24 hours, secreted embryonic alkaline phosphatase (SEAP) activity was detected by QUANTI-Blue Solution (InvivoGen, Cat. rep-qbs).

Statistical analysis

All data were expressed as mean ± SE of mean (SEM). Statistical analysis was performed with SPSS 20.0 software. The Student *t* test was used after the normal distribution test when 2 groups were compared. If normality or homogeneity of variance was not met, the

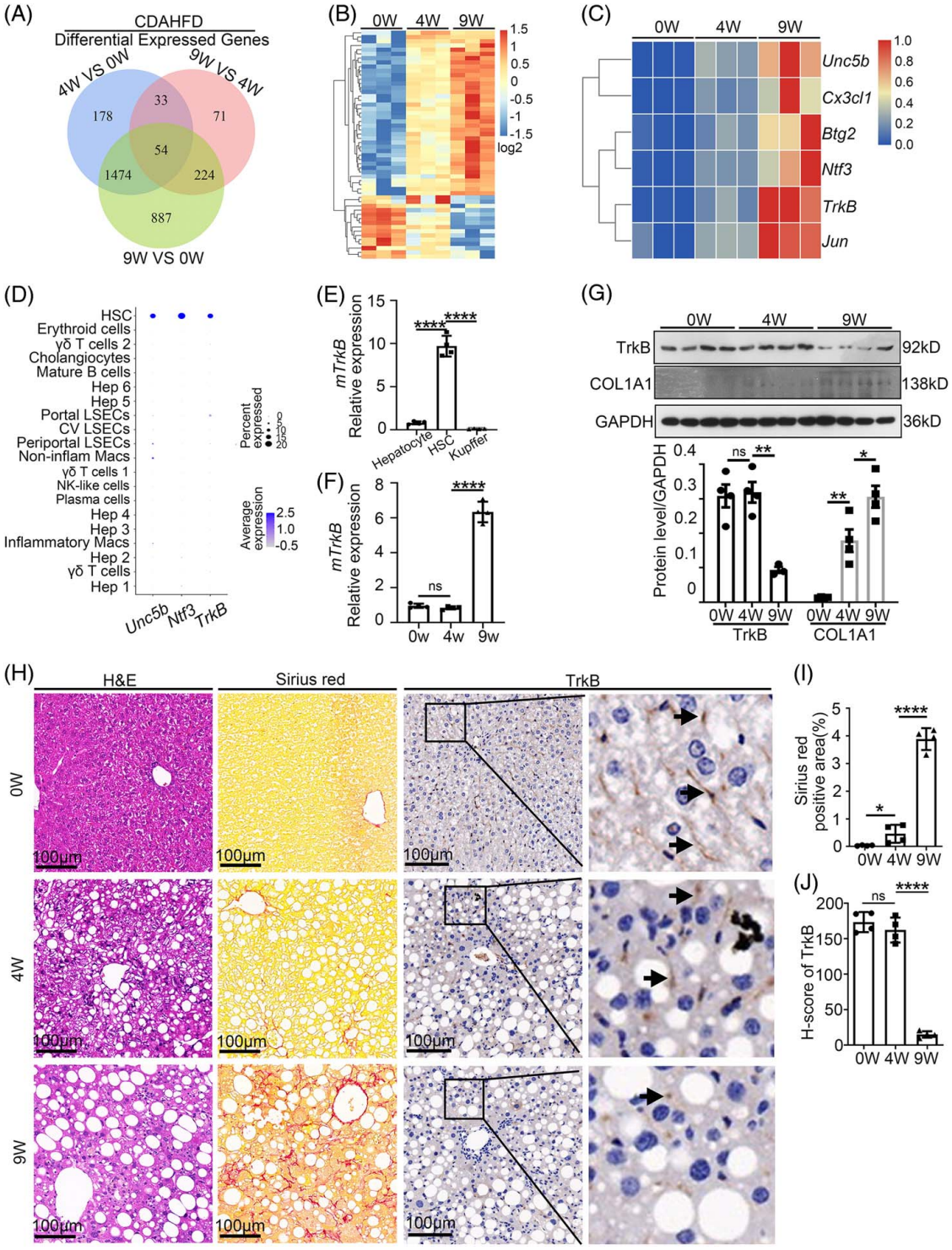

FIGURE 1 Abnormal TrkB expression during the progression of CDAFHD-induced hepatic fibrosis. (A) Venn diagram showing the overlap of DEGs ($|Log_2FC| \geq 1.5$) in the comparison sets of 3 CDAFHD-induced liver fibrosis stages (4 vs. 0 wk, 9 vs. 4 wk, 9 vs. 0 wk). (B) The heat map was generated by TBtools showing the expression levels that cochanged in all 3 comparisons. (C) A set of central nervous system genes that cochanged in (B). (D) Seurat Dotplot showing the expression level of *Unc5b*, *Ntf3*, and *TrkB* in each cluster by single-cell RNA sequencing (scRNA-seq) in GSE115469. The dot size represents the percentage of the cell expressing the gene, and the dot color represents the average expression of interested genes in clusters. (E) Relative *TrkB* expression level detected by quantitative reverse transcriptase PCR (qRT-PCR) in primary mouse cells. (F) Relative expression of *TrkB* detected by qRT-PCR in HSC cells isolated from CDAFHD-fed mice collected at 0, 4, and 9 weeks, n = 3 per group. (G) Western blot analysis showed the protein levels of TrkB and COL1A1 in liver samples from normal and CDAFHD-fed mice. GAPDH was used for internal control, n = 4 per group. (H) Representative images of H&E and Sirius Red staining and immunohistochemical (IHC) of TrkB. The arrow indicated positive TrkB staining on the cell membrane. Scale bars, 100 μm. (I) Quantification of Sirius Red staining in (H). (J) H-score values of TrkB in (H). n = 4 per group. Data were mean ± SEM. For (E), (F), (G), (I), and (J), significance was determined by the ANOVA test (*$p < 0.05$, **$p < 0.01$, ***$p < 0.001$, ****$p < 0.0001$). Abbreviations: H&E, hematoxylin and eosin; TrkB, tyrosine kinase receptor.

Mann-Whitney *U* test was used to compare the 2 groups. When the experimental design involves more than 2 groups, the ANOVA was used to compare between groups after the normal distribution test, and multiple comparisons between 2 given groups were completed by the least significant difference test. Supposing normality or homogeneity of variance was not met. In that case, the Kruskal-Wallis test was used to compare between groups, and multiple comparisons between 2 given groups were completed by the Hodges-Lehmann test. A value of $p < 0.05$ was considered to be statistically significant. *p*-values are shown as $*p < 0.05$, $**p < 0.01$, $***p < 0.001$, and $****p < 0.0001$.

Detailed methods are presented in Supplemental Material, primers and drugs used are provided in Supplemental Tables S2–4 (http://links.lww.com/HEP/D445).

RESULTS

Abnormal TrkB expression during the progression of hepatic fibrosis

NASH patients with fibrosis are associated with significantly shortened survival negatively with the severity of fibrotic extent.[15] To identify novel therapeutic targets regulating the progression of liver fibrosis, whole-transcriptome expression profile analysis was performed in liver samples from CDAHFD-fed mice at 0, 4, and 9 weeks (Figure S1A–D, http://links.lww.com/HEP/D445). Only 87 genes overlapped between 4W versus 0W (1739 differentially expressed genes) and 9W versus 4W (382 differentially expressed genes) (Figure S1E, http://links.lww.com/HEP/D445), suggesting that elaborate genes could be switched on or off during the progression of liver fibrosis. Compared with the differentially expressed genes in human HSCs measured at a single-cell resolution[16] (Figure S1E, http://links.lww.com/HEP/D445), most genes reported were considered to function as the regulator of fibrosis, except *Fmo3*, *TrkB*, and *Celf1* (Figure S1F, http://links.lww.com/HEP/D445). Meanwhile, 54 overlapped genes were discovered between 4W versus 0W, 9W versus 4W, and 9W versus 0W data sets (Figure 1A, B). In speculation, these 54 genes participated in regulating lipid metabolism and hepatic fibrosis at the same time. Interestingly, among them, a set of genes were found to participate in neuronal functions, such as *TrkB*, *Ntf3*, *Unc5b*, *Cx3cl1, Btg2*, and *Jun* (Figure S2, http://links.lww.com/HEP/D445, Figure 1C). *Cx3cl1, Btg2*, and *Jun* were reported to participate in the regulation of hepatic function and fibrosis.[17,18] Gene Expression Omnibus database indicated that *TrkB*, *Ntf3*, and *Unc5b* were specifically expressed in human HSCs (Figure 1D). The specific expression of *mTrkB* and *mUnc5b* in primary mouse HSCs was confirmed by RT-PCR (Figure 1E, Figure S3A, B, http://links.lww.com/HEP/D445). Meanwhile, *mTrkB*, *mUnc5b*, and *mNTF3* were enhanced in HSCs during fibrotic progression in CDAHFD-fed mice (Figure 1F, Figure S3C, D, http://links.lww.com/HEP/D445). These RNA sequencing results pointed to an assumption that TrkB might be a key component in regulating hepatic fibrosis. It has been reported that TrkB mutation leads to obesity in humans and mice[13,19]; however, how TrkB is involved at a molecular level in liver fibrosis remains poorly understood.

Subsequently, it was found that TrkB protein level was significantly reduced at a late stage of NASH-fibrosis in CDAHFD-fed mice (9 wk) (Figure 1G). Histologically, TrkB protein levels decreased markedly at 9 weeks in liver sections, in contrast to an increased collagen deposition (Figure 1H–J). Furthermore, immunofluorescent staining confirmed that TrkB expression was relatively lower at 9 weeks in liver sections than early stages of this murine NASH model (Figure S4, http://links.lww.com/HEP/D445).

After that, TrkB expression was determined in the CCl_4-induced liver fibrosis model. Histologically, the TrkB protein level decreased (Figure 2A, D), whereas significant fibrotic progression was visualized by Sirius red and α-SMA immunohistochemical staining at 0, 4, and 8 weeks (Figure 2A–C). Consistent with CDAHFD-fed mice, quantitative reverse transcriptase PCR and western blotting analyses verified an increased TrkB transcript but diminished protein level in the CCl_4-induced fibrotic model (Figure 2E, F). Moreover, downregulated TrkB protein was found in human fibrotic livers by immunohistochemical staining (Figure 2G), whereas Gene Expression Omnibus database indicated upregulated transcripts in human cirrhotic livers (Figure 2H, I). All of these results demonstrated that TrkB expression was altered during the progression of hepatic fibrosis in both animal models and chronic liver diseases in human.

TrkB inhibited HSC proliferation and activation *in vitro*

To further reveal the function of TrkB in HSCs, TrkB was overexpressed in human HSC LX2 cells by lentiviral transduction (Figure 3A). CCK8 assay was conducted, and the results indicated that TrkB overexpression significantly resulted in a decrease in HSC proliferation (Figure 3B). Flow cytometry data showed that TrkB overexpression inhibited G1/S phase transition (Figure 3C, D). G1/S-specific transcripts, such as *E2F2*, *MCM10*, *CDT1*, and *CCND3*, were highly repressed (Figure 3E). Cyclin-dependent kinase (CDK) activity is essential to the G1/S phase transition. Western blot assay confirmed that CDK2 and CDK6 were downregulated when TrkB was overexpressed in LX2 cells (Figure 3F). On the contrary, LX2 cell proliferation was enhanced when TrkB was inhibited by shRNA

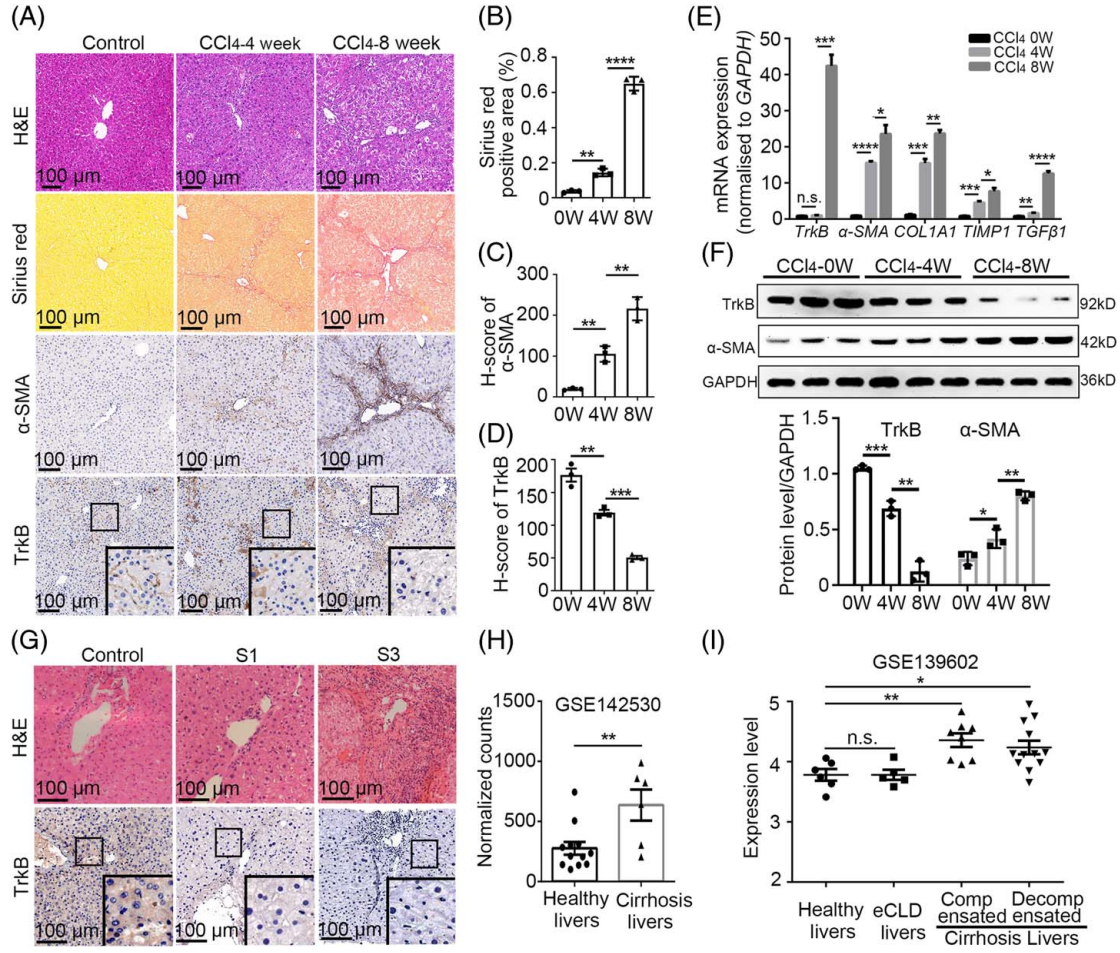

FIGURE 2 TrkB expression during fibrotic progression induced by CCl_4 injection. (A) Representative images of H&E, Sirius Red, and immunohistochemical staining (IHC) of α-SMA and TrkB in CCl_4-induced mouse fibrosis models. Scale bars, 100 μm. (B) Quantification of Sirius Red staining in (A). n = 3 per group. H-score values of α-SMA (C) and TrkB (D) in (A). n = 3 per group. (E) Relative expression of *TrkB*, *α-SMA*, *COL1A1*, *TIMP1*, and *TGF-β1* was detected by quantitative reverse transcriptase PCR in liver samples of CCl_4-induced mice collected at 0, 4, and 8 weeks, n = 3 per group. (F) Western blot analysis showed the protein levels of TrkB and α-SMA in liver samples from CCl_4-treated mice collected at 0, 4, and 8 weeks. GAPDH was used for internal control, n = 3 per group. (G) Representative images of H&E and IHC staining of TrkB in human liver tissues. Scale bars, 100 μm. (H and I) Relative TrkB mRNA levels in GEO data sets. Data were mean ± SEM. For (B), (C), (D), (E), (F), and (I), significance was determined by the ANOVA test. For (H), significance was determined by the Student *t* test. (*$p < 0.05$, **$p < 0.01$, ***$p < 0.001$, ****$p < 0.0001$). Abbreviations: CCl_4, carbon tetrachloride; H&E, hematoxylin and eosin; ns, not significant; TrkB, tyrosine kinase receptor.

lentiviral vector transduction (Figure S5A, B, http://links.lww.com/HEP/D445). Accordingly, TrkB knockdown in LX2 cells accelerated the G1/S phase transition with increased CDK2 protein level and *E2F2*, *CDT1*, and *CCND3* transcripts (Figure S5C–F, http://links.lww.com/HEP/D445). However, TrkB overexpression or knockdown did not affect the apoptosis of LX2 cells (Figure S6A–D, http://links.lww.com/HEP/D445). Furthermore, to imitate *in vivo* properties of the liver, the 3D liver spheroids model were established using HepG2-red fluorescent protein (GFP) and LX2-green fluorescent protein (GFP), LX2-TrkB-GFP, and LX2-TrkB-sh2-GFP cells (Figure 3G-H). ATP detection reagent was used to measure 3D liver spheroid viability, and it was evident that TrkB overexpression in HSCs markedly inhibited the growth of 3D liver spheroids (Figure 3I).

It is well-known that TGF-β is a potent fibrogenic cytokine. TrkB overexpression obligated TGF-β1–induced COL1A1 production in HSCs as evidenced by western blot assay (Figure 3J). Quantitative reverse transcriptase PCR analysis confirmed that TrkB overexpression repressed TGF-β1–induced upregulation of COL1A1 and CTGF mRNA levels in LX2 cells (Figure 3K, L). The production of α-SMA and COL1A1 in 3D liver spheroids was induced after palmitic acid (PA) treatment; however, this effect was counteracted when TrkB was overexpressed in LX2 cells, as evidenced by western blot and RT-PCR analyses (Figure 3M–O). Accordingly, TrkB knockdown facilitated HSC activation (Figure S7A–C, http://links.lww.com/HEP/D445). In summary, TrkB overexpression inhibited HSC proliferation and activation *in vitro* stimulated by TGFβ1 or saturated fatty acid overload.

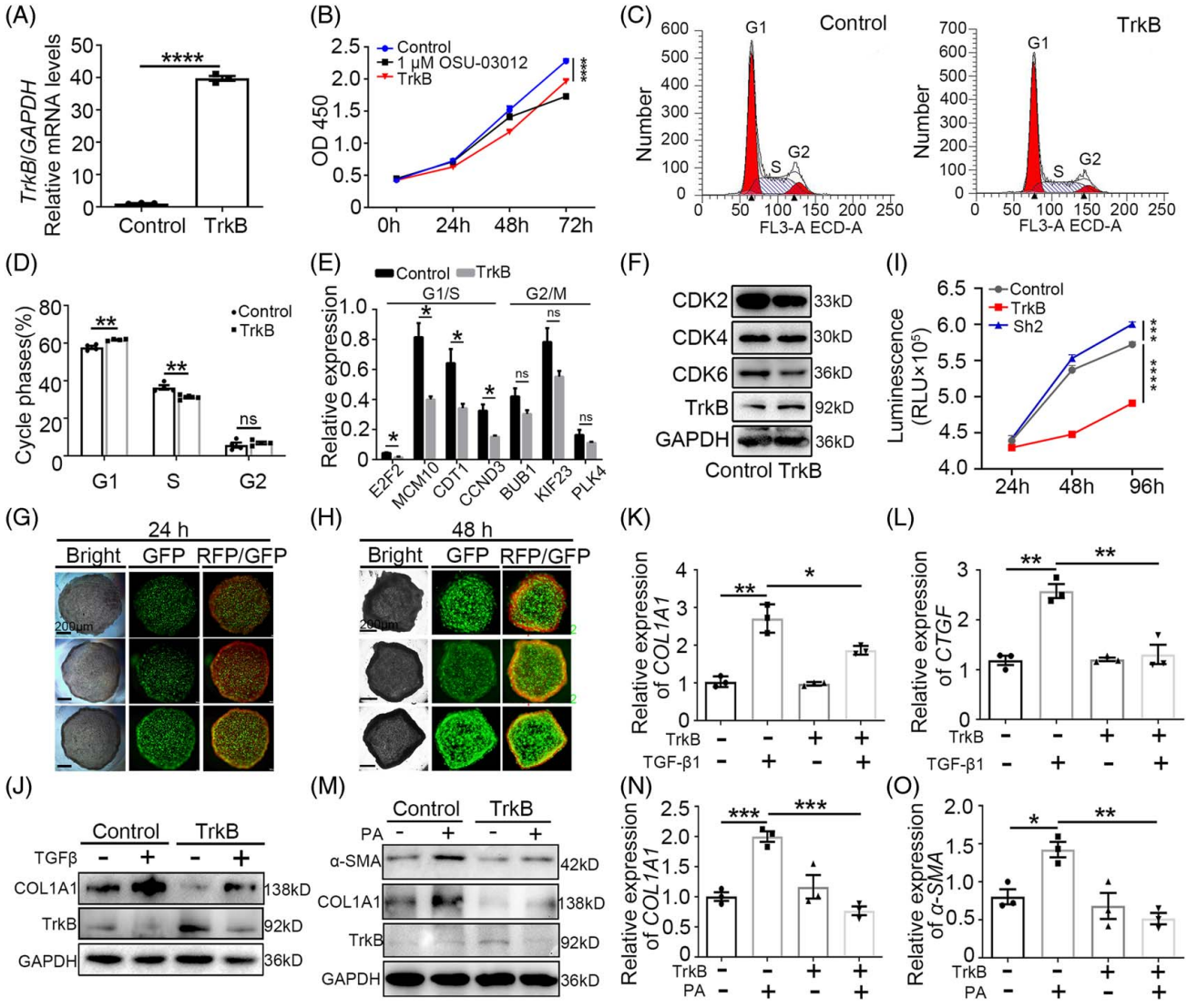

FIGURE 3 TrkB inhibited HSC and 3-dimensional (3D) liver spheroid proliferation and activation *in vitro*. (A) LX2 cells were infected with Lentivirus-Con and Lentivirus-TrkB and then *TrkB* expression in LX2 cells was confirmed through quantitative reverse transcriptase PCR (qRT-PCR). (B) Cell proliferation evaluation of LX2 cells using the CCK8 assay. OSU-03012 at 1 μM was used as a negative control, n = 6 per group. (C and D) Cell cycle distribution was measured by flow cytometry in control and LX2-TrkB cells, n = 4 per group. (E) Expression of cell cycle–associated genes was compared between control and LX2-TrkB cells by qRT-PCR. (F) Protein levels of CDK2 (cyclin-dependent kinase 2), CDK4 (cyclin-dependent kinase 4), and CDK6 (cyclin-dependent kinase 6) in control and LX2-TrkB cells, as determined by western blot analysis. (G and H) HepG2-red fluorescent protein (GFP) cells were cultured with LX2-green fluorescent protein (GFP) (up), LX2-TrkB-GFP (middle), and LX2-TrkB-sh2-GFP (down), respectively, to construct 3D spheroids for 24 hours (G) and 48 hours (H) in the medium. Scale bars, 200 μm. (I) Spheroid proliferation evaluation of HepG2-LX2 3D spheroids using luminescent cell health assay, n = 5 per group. (J) Western blot analysis of COL1A1 in control and LX2-TrkB cells treated with or without TGF-β (10 ng/mL) for 24 hours. qRT-PCR analysis of *COL1A1* (K) and *CTGF* (L) in control and LX2-TrkB cells treated with or without TGF-β (10 ng/mL) for 24 hours, n = 3 per group. (M) Western blot analysis of COL1A1, α-SMA, TrkB in control, and LX2-TrkB cells treated with or without PA (0.5 mM) for 24 hours. (N and O) qRT-PCR analysis of *COL1A1*, *α-SMA* in control, and LX2-TrkB cells treated with or without PA (0.5 mM) for 24 hours, n = 3 per group. Data are mean ± SEM. For (A), (D), and (E), significance was determined by Student *t* test. For (B), (I), (K), (L), (N), and (O), significance was determined by the ANOVA test (*$p < 0.05$, **$p < 0.01$, ***$p < 0.001$, ****$p < 0.0001$). Abbreviations: CCl_4, carbon tetrachloride; H&E, hematoxylin and eosin; TrkB, tyrosine kinase receptor.

TrkB suppressed the TGF-β1–induced signaling pathways in HSCs

TrkB phosphorylation is crucial for various growth activities.[20] To investigate the molecular link between TrkB and HSCs, LX2 cells were treated with a TrkB agonist 7, 8-dihydroxyflavone (7, 8-DHF).[21] It appeared that HSC proliferation and activation were not affected by 7, 8-DHF treatment (Figure S8A–D, http://links.lww.com/HEP/D445), suggesting that TrkB phosphorylation did not directly affect HSC function.

Thereafter, RNA sequencing analysis in LX2 cells determined the gene expression profile in response to TrkB overexpression. As shown in Figure 4A, 1855 upregulated and 1509 downregulated genes were identified. A set of genes encoding collagen alpha

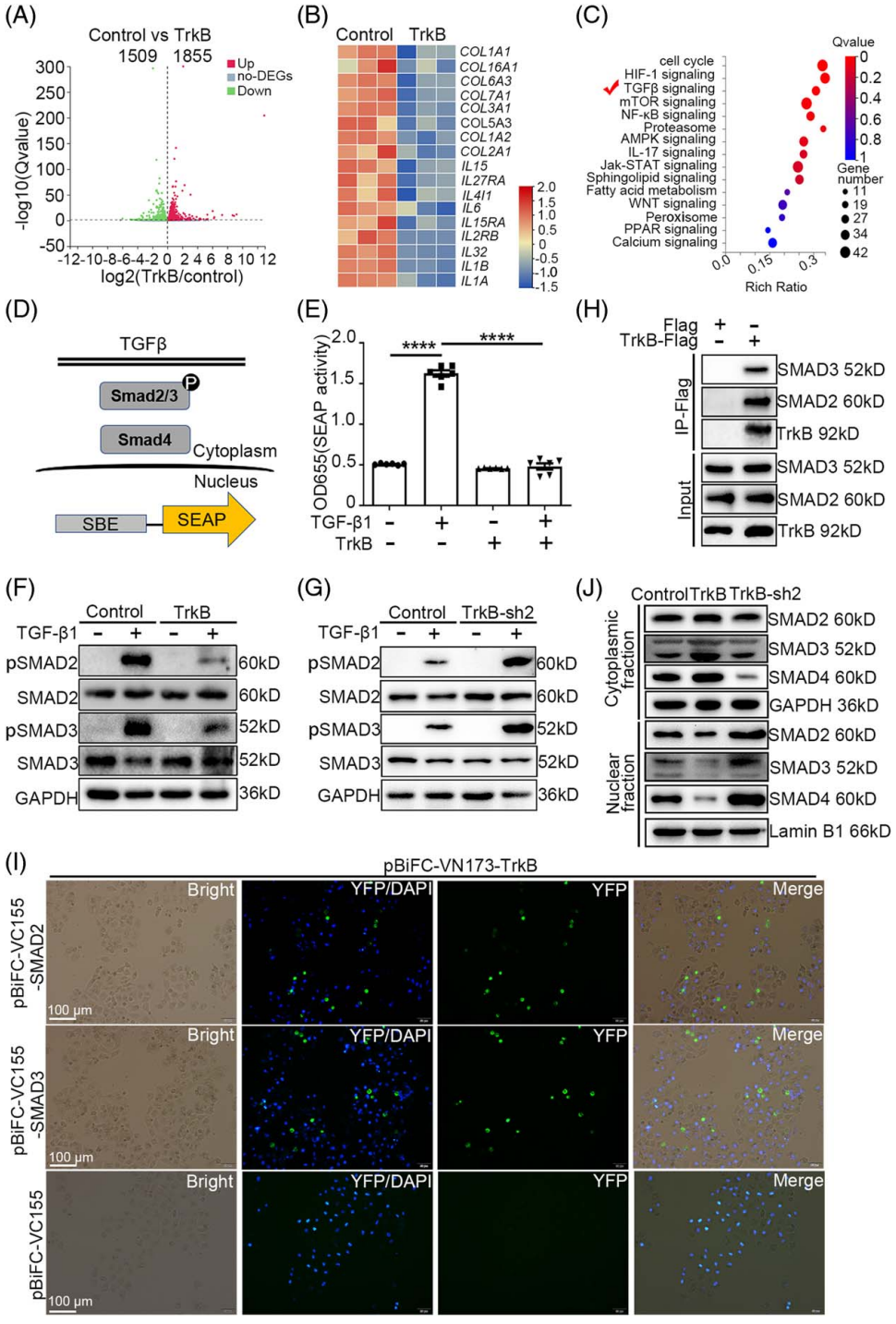

FIGURE 4 TrkB suppressed the TGF-β1–induced signaling pathways in HSCs. (A) Volcano plots. The red dots represented upregulated genes and the green dots represented downregulated genes in control and LX2-TrkB cells. (B) Heat map was generated by TBtools showing the expression levels of collagen and *interleukin genes* in control and LX2-TrkB cells. (C) KEGG Pathway enrichment analysis of transcriptome in control and LX2-TrkB cells. (D) Schematic diagram of human TGF-β SEAP reporter cells. (E) SEAP activity analysis of control and LX2-TrkB cells treated with or without TGF-β (10 ng/mL) for 24 hours, n = 6 per group. Data were mean ± SEM (****$p < 0.0001$; ANOVA test). (F and G) Western blot analysis of SMAD2/3 and pSMAD2/3 in control, LX2-TrkB and LX2-TrkB-sh2 cells treated with or without TGF-β (10 ng/mL) for 24 hours. (H) Co-IP analysis to evaluate the interaction between TrkB and SMAD2/3 in LX2 using endogenous Flag-TrkB. (I) BiFC (Bimolecular Fluorescence Complementation) analysis of the interaction between TrkB and SMAD2/3 in hepatocytes. (J) Western blot analysis of the translocation of SMAD2/3/4 in control, LX2-TrkB, and LX2-TrkB-sh2 cells. Abbreviations: DEGs, differentially expressed gene; TrkB, tyrosine kinase receptor; YFP, yellow fluorescent protein.

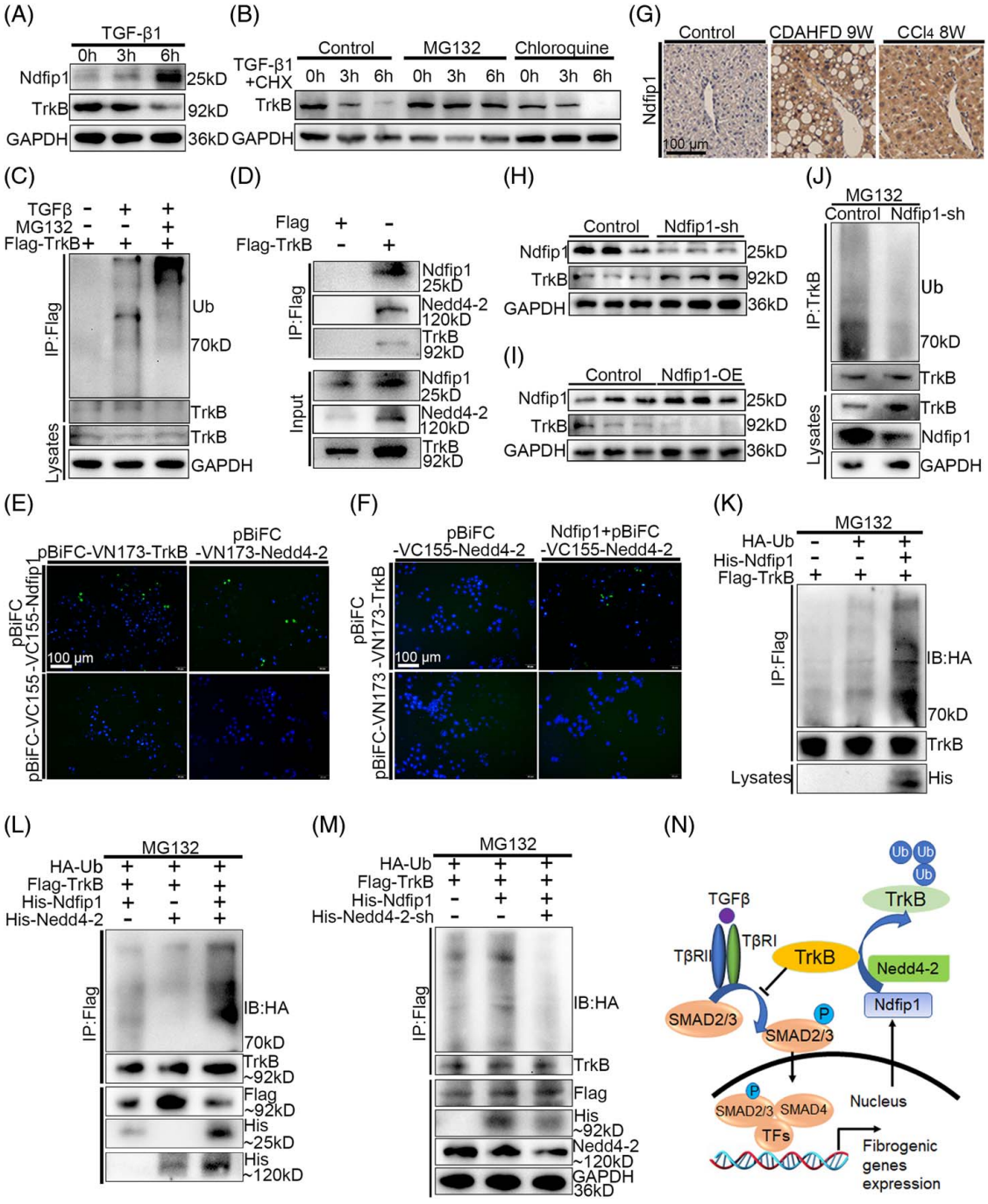

FIGURE 5 TGF-β1–induced Ndfip1 promoted TrkB degradation through the ubiquitin-proteasome pathway. (A) Representative images of Western blotting showed the expression level of TrkB and Ndfip1 in HSCs treated with TGF-β (10 ng/mL). (B) Representative blotting images for TrkB expression in HSCs treated with cycloheximide (CHX, 10 μM), together with MG132 (10 μM) or chloroquine (20 μM). (C) Representative blotting images for ubiquitinated TrkB in HSCs. (D) Representative co-IP analysis evaluating the interaction between TrkB and Nedd4-2, Ndfip1 in HSCs using exogenous Flag-TrkB, Flag vector was used as control. (E and F) BiFC analysis of the interaction between Ndfip1, TrkB, and Nedd4-2. Scale bars, 100 μm. (G) Representative immunohistochemical images of Ndfip1 staining in liver samples of CDAHFD-fed and CCl_4-treated mice. Scale bars, 100 μm. Representative blotting images for TrkB expression in Ndfip1-sh HSCs (H) and Ndfip1-overexpressed HSCs (I). Representative blotting images for ubiquitinated TrkB in Ndfip1-sh HSCs (J) and Ndfip1-overexpressed HSCs (K). (L) Ubiquitination assay showed the TrkB ubiquitination induced by the coexpression of Ndfip1 and Nedd4-2 (lane 3) compared with Nedd4-2 (lane 2). (M) Ubiquitination assay showed the TrkB ubiquitination repressed by knockdown of Nedd4-2 (lane 3) when coexpressed with Ndfip1. (N) Working model depicting how TrkB regulates the progression of liver fibrosis through the TGF-β/SMADs pathway. TrkB inhibited the TGF-β/SMADs pathway by directly interacting with SMADs proteins and repressed SMADs nuclear retention in HSCs. TGF-β–induced Ndfip1 promoted the ubiquitination and proteasomal degradation of TrkB during HSC activation through E3 ligase Nedd4-2. Abbreviations: BiFC, bimolecular fluorescence complementation; Ndfip1, Nedd4 family interacting protein-1; TrkB, tyrosine kinase receptor.

proteins and cytokines were downregulated in TrkB-overexpressed LX2 cells (Figure 4B), indicating its inhibitory effects on extracellular matrix formation. Gene Ontology analysis revealed that TrkB mainly affected the TGF-β signaling pathway in HSCs (Figure 4C). As shown in Figure S9 (http://links.lww.com/HEP/D445), the expression of TGF-β signaling components (*PAI1*, *SMAD7*, and *ACVR1C*) was affected in *TrkB*-overexpressed or knocked down LX2 cells after TGF-β treatment. Then, the HEK-Blue TGF-β cells were used to monitor the activity of the TGF-β/SMAD signaling pathway, in which TGF-β treatment elicited phosphorylated SMAD3/4 binding to SMAD-binding domain of downstream-secreted alkaline phosphatase (SEAP), and lead to increased activity of SEAP, as illustrated in Figure 4D. Obviously, TGF-β1–induced SEAP activity was repressed by overexpressing TrkB (Figure 4E). Coimmunoprecipitation analysis demonstrated that TrkB failed to interact with TGF-β receptors TGFBR1 and TGFBR2 (Figure S10, http://links.lww.com/HEP/D445); however, the phosphorylation of SMAD2/3 stimulated by TGF-β1 was significantly abrogated in TrkB-overexpressed LX2 cells (Figure 4F); in contrast, it was enhanced in TrkB–knocked-down LX2 cells (Figure 4G). In addition, the direct interaction between TrkB and SMAD2/3 was confirmed by the coimmunoprecipitation assay in LX2 cells (Figure 4H). Furthermore, TrkB and SMAD2/3 were fused with 2 fragments of yellow fluorescent protein, respectively. Bimolecular fluorescence complementation (BiFC) assay was performed to visualize direct interactions between TrkB and SMAD2/3 proteins (Figure 4I). Strong fluorescent signals were observed when pBiFc-VN173-TrkB was coexpressed with pBiFC-VC155-SMAD2/3 compared with control, indicating a direct interaction between TrkB and SMAD2/3 *in vivo* (Figure 4I). Subsequently, weak and few fluorescent signals were detected when cotransfected pBiFc-VN173-TrkB-N (N-terminal) with pBiFC-VC155-SMAD2/3. In contrast, strong fluorescent signals appeared when cotransfected pBiFc-VN173-TrkB-KD (Kinase Domain) with pBiFC-VC155-SMAD2/3 (Figure S11A–D, http://links.lww.com/HEP/D445), indicating that the TrkB kinase domain is essential for the interaction with SMADs. Moreover, the TrkB kinase domain was able to bind directly to both the MH1 (Mad homology 1) and MH2 (Mad homology 2) regions of SMAD2/3 (Figure S11C, D). TrkB overexpression increased cytoplasmic protein levels of SMADs and repressed nuclear retention of SMADs in HSCs (Figure 4J). On the contrary, the SMAD2/3 protein level was decreased in the cytosolic fraction but enhanced in the nuclear protein extract when TrkB was knocked down in HSCs (Figure 4J). These results indicated that TrkB was a negative regulator involved in TGF-β/SMAD signaling. The overexpression of TrkB dramatically suppressed the nuclear translocation of SMADs, thereby negatively transcribing the downstream genes.

TGF-β1–stimulated Ndfip1 expression promoted TrkB degradation through the ubiquitin-proteasome pathway

Additional efforts were made to delineate how the TrkB expression affects TGF-β/SMAD signaling pathway. First, LX2 cells were treated with TGF-β, and TrkB gradually decreased over time under TGF-β exposure in these cells (Figure 5A). TrkB degradation was blocked with the treatment of a proteasome inhibitor MG132. In contrast, the addition of a lysosome inhibitor, chloroquine, had little impact on TrkB content (Figure 5B). Subsequently, it was found that TrkB was ubiquitinated after TGF-β treatment. This effect was decreased after the addition of MG132 (Figure 5C). These observations suggested that the degradation of TrkB was mediated by a ubiquitin-proteasome pathway during HSC activation. In a previous study, it was reported that Ndfip1 promoted TrkB ubiquitination through the recruitment of Nedd4-2.[22] Thereby, an immunoprecipitation assay was conducted in LX2-Flag and LX2-TrkB-Flag cells. Of note, both Ndfip1 and Nedd-2 were pulled down after protein lysates were purified with antiflag affinity gel (Figure 5D). Furthermore, it was observed that Ndfip1 interacted directly with TrkB and Nedd4-2 in hepatocytes by a BiFC assay (Figure 5E). However, TrkB did not interact with Nedd4-2 when Ndfip1 was absent (Figure 5F). These data indicated that Ndfip1 might act as a "bridge" between TrkB and Nedd4-2 and was essential for the critical role of TrkB in the TGF-β/SMAD signaling pathway.

Ndfip1 is a protein that functions as an adaptor of the Nedd4 family, and its level was significantly increased in LX2 cells under TGF-β stimulation (Figure 5A). Increased Ndfip1 was detected in both murine models of hepatic fibrosis at 9 weeks in CDAHFD-fed mice or 8 weeks of CCl_4 intoxication (Figure 5G). To further elucidate the function of Ndfip1 in the TGF-β/SMAD signaling pathway, lentiviral vectors for overexpression and knocked-down were constructed and transduced in LX2 cells. Western blot assay revealed that TrkB was increased when Ndfip1 was knocked-down, whereas it was highly decreased in Ndfip1-overexpressed cells (Figure 5H, I). Consistently, Ndfip1 knockdown significantly repressed the ubiquitination of endogenous TrkB in HSCs, and Ndfip1 overexpression markedly promoted exogenous TrkB ubiquitination (Figure 5J, K), indicating that TrkB ubiquitination was dependent on Ndfip1. In addition, compared with overexpression with Ndfip1 or Nedd4-2 alone, much more ubiquitinated TrkB was detected when Nedd4-2 was coexpressed with Ndfip1 (Figure 5L). As expected, the ubiquitination of TrkB promoted by Ndfip1 overexpression was notably inhibited when Nedd4-2 was knocked-down (Figure 5M). In summary, TGF-β–stimulated Ndfip1 expression enhanced the ubiquitination of TrkB through Nedd4-2 in HSCs, as illustrated in Figure 5N.

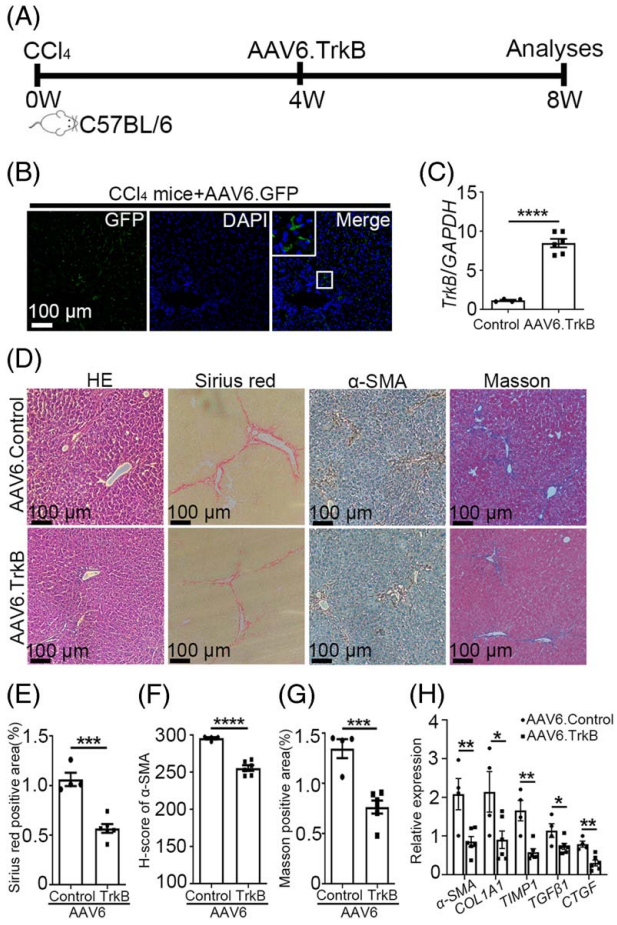

FIGURE 6 AAV6-mediated TrkB delivery inhibited CCl_4-induced liver fibrosis. (A) Schematic overview of the experiments ($n_{AAV6.control}$ = 4, $n_{AAV6.TrkB}$ = 6). (B) AAV6.GFP immunofluorescence in liver samples from CCl_4-treated mice. Scale bars, 100 μm. (C) *TrkB* expression in liver samples from CCl_4-treated mice was confirmed through quantitative reverse transcriptase PCR (qRT-PCR). (D) Representative images of H&E, Sirius Red and Masson, and immunohistochemical staining of α-SMA. Scale bars, 100 μm. (E) The quantification of Sirius Red staining in (D). H-score values of α-SMA (F) and quantification of Masson staining (G) in (D). (H) qRT-PCR analysis of *COL1A1*, *α-SMA*, *TIMP1*, *TGF-β1*, and *CTGF* in CCl_4-treated liver samples of AAV6.control and AAV6.TrkB. Data were mean ± SEM (*$p < 0.05$, **$p < 0.01$, ***$p < 0.001$, ****$p < 0.0001$; Student *t* test). Abbreviations: AAV6, adeno-associated virus vector serotype 6; CCl_4, carbon tetrachloride; HE, hematoxylin and eosin; TrkB, tyrosine kinase receptor.

AAV6-mediated TrkB delivery ameliorated CCl_4-induced liver fibrosis *in vivo*

Furthermore, the effects of TrkB were examined in the CCl_4-induced fibrosis model in mice by its overexpression with the AAV-medicated gene delivery (Figure 6A). AAV6 vector has been identified with relatively high myofibroblast tropism in mouse liver[23]; therefore, the AAV6-TrkB vector was selected to investigate the role of TrkB during fibrotic progression. Mice injected with AAV6-GFP were used as controls. GFP fluorescent signal was observed in the liver in histological examination (Figure 6B), indicating successful transduction after i.v. AAV6 injection. As confirmed by quantitative reverse transcriptase PCR, TrkB transcript was significantly increased in AAV6-TrkB–injected mice (Figure 6C). Histologically, a considerable reduction of fibrosis was confirmed in AAV6-TrkB–injected mice, as shown by α-SMA, Sirius Red, and Masson staining (Figure 6D-G). The expression of fibrogenic genes, such as *α-SMA*, *COL1A1*, *TIMP1*, *TGF-β*, and *CTGF*, was dramatically repressed in AAV6-TrkB–injected mice (Figure 6H). These results indicated that TrkB overexpression ameliorated CCl_4-induced hepatic fibrosis in mice. Furthermore, it was found that phosphorylated SMAD2/3 were significantly suppressed in AAV6-TrkB–injected livers (Figure S12, http://links.lww.com/HEP/D445), confirming a negative regulation of TGF-β signaling in this mouse model of hepatic fibrosis.

Overexpression of TrkB in hepatocytes suppressed inflammation and fibrogenesis

Hepatocytes act as the regulator of HSC activation, as hepatocellular injury is an initial and persistent factor for liver fibrosis.[24] Thus, TrkB was overexpressed in HepG2 cells to examine its protective effects. First, it was observed that TGF-β–induced SMAD3 phosphorylation was repressed when TrkB was overexpressed in HepG2 cells (Figure S13A, B, http://links.lww.com/HEP/D445), unveiling the blockade of TGF-β signaling in hepatocytes. TrkB considerably inhibited the expression of inflammation contributor CD36 and inflammatory cytokines (*IL-1b*, *TNF-α*, and *IL-6*) in PA-overloaded HepG2 cells (Figure S13C, S14A–D, http://links.lww.com/HEP/D445) for determining the *in vitro* anti-inflammatory activity of TrkB. Then HSCs were incubated with a conditioned medium from HepG2 cells treated with PA for 24 hours (Figure S14A, http://links.lww.com/HEP/D445). Upregulated fibrogenic genes (*COL1A1, α-SMA, TIMP1*, and *TGF-β*) on exposure to conditioned medium from PA-treated HepG2 were suppressed in the medium derived from TrkB-activated HepG2 cells (Figure S14E–H, http://links.lww.com/HEP/D445). These data illustrated that TrkB overexpression was beneficial to hepatocellular injury *in vitro*.

AAV8-mediated TrkB delivery attenuated NASH-associated liver fibrosis in mice

Given a low level of NASH-induced fibrosis and inefficient myofibroblast tropism of AAV6, AAV8 vectors were administered in CDAHFD-fed mice to investigate the function of TrkB during fibrotic progression (Figure 7A). GFP signals were clearly observed in liver sections after AAV8-GFP injection (Figure 7B), and TrkB transcript was markedly upregulated in AAV8-TrkB–injected mouse liver (Figure 7C), indicating the

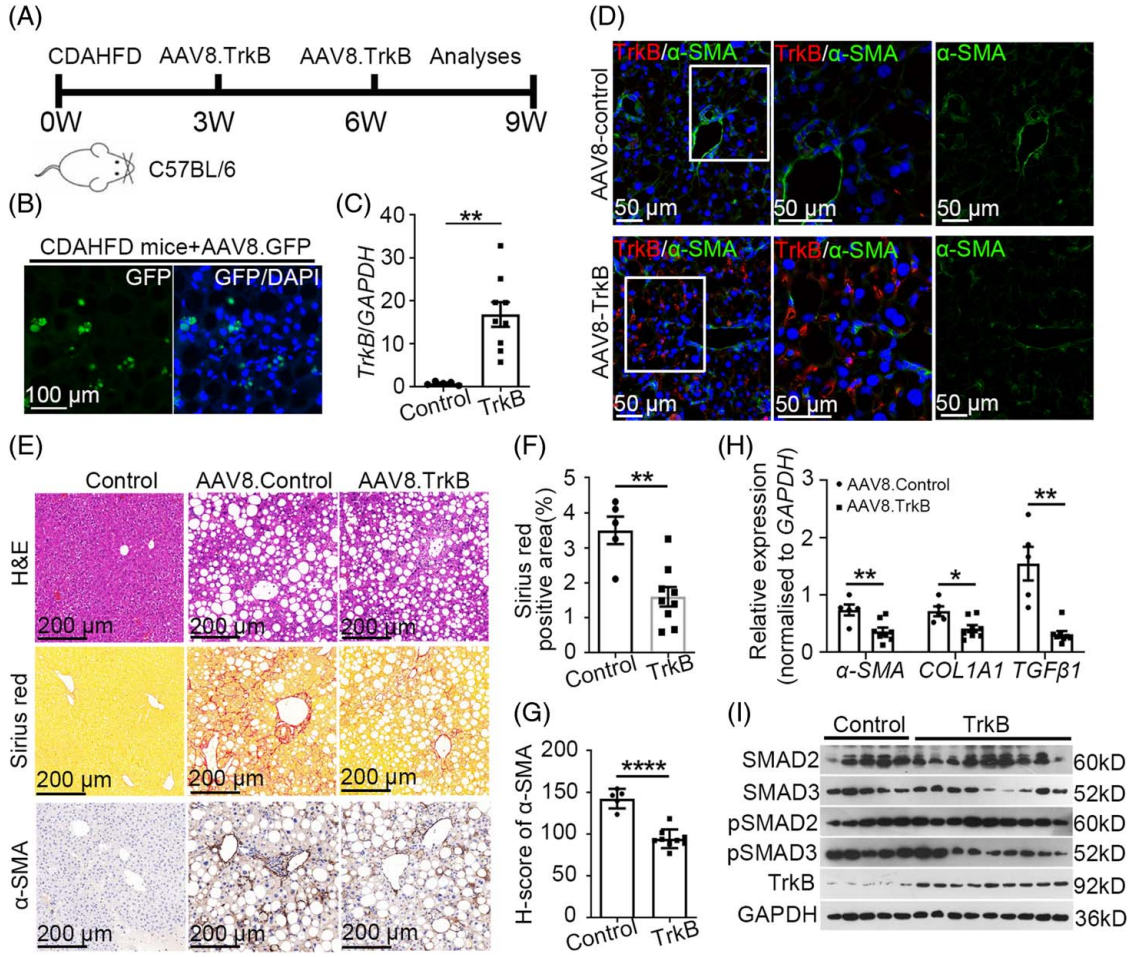

FIGURE 7 AAV8-mediated TrkB delivery inhibited CDAHFD-induced liver fibrosis. (A) Schematic overview of the experiments ($n_{AAV8.control}$ = 5, $n_{AAV8.TrkB}$ = 9). (B) AAV8.GFP immunofluorescence in liver samples from CDAHFD-fed mice. Scale bars, 100 μm. (C) *TrkB* expression in liver samples from AAV8.control and AAV8.TrkB–injected mice were confirmed through quantitative reverse transcriptase PCR (qRT-PCR). (D) TrkB and α-SMA co-immunofluorescence in liver samples from AAV8.control and AAV8.TrkB-injected mice. Scale bars, 100 μm. (E) Representative images of H&E and Sirius Red and immunohistochemical staining of α-SMA. Scale bars, 100 μm. (F) Quantification of Sirius Red staining in (E). (G) H-score values of α-SMA in (E). (H) qRT-PCR analysis of *COL1A1*, *α-SMA*, and *TGF-β* in CDAHFD-fed liver samples of AAV8.control and AAV8.TrkB–injected mice. (I) Representative images of western blot analysis of SMAD2/3 and pSMAD2/3 in AAV8.control and AAV8.TrkB–injected mice. Data were mean ± SEM; (*$p < 0.05$, **$p < 0.01$, ***$p < 0.001$, ****$p < 0.0001$; Student *t* test). Abbreviations: AAV8, adeno-associated virus vector serotype 8; HE, hematoxylin and eosin; TrkB, tyrosine kinase receptor.

efficient transduction of AAV8 vectors. Next, Sirius red staining, IF, and IHC analysis of α-SMA showed that liver fibrosis was significantly reduced in AAV8-TrkB–injected mice (Figure 7D–G). The expression of fibrogenic genes, such as *α-SMA*, *COL1A1*, and *TGF-β*, was strikingly suppressed in the livers of AAV8-TrkB–injected plus CDAHFD-fed mice for 9 weeks (Figure 7H). These results indicated that TrkB overexpression in hepatocytes after AAV8 delivery attenuated CADHFD-induced hepatic fibrosis in mice. In addition, phosphorylated SMAD3 was significantly repressed in the liver of AAV8-TrkB–injected mice (Figure 7I), suggesting a negative regulation of TGF-β signaling in this murine model of NASH fibrotic progression. Similar results were observed in AAV8-delivered ob/ob-NASH mice (Figure S15). Interestingly, it was evident that TrkB prevented caspase-3 activation in CDAHFD-fed mice but not in ob/ob-NASH mice (Figure S16, http://links.lww.com/HEP/D445), probably because CDAHFD had profound liver toxicity and induced more pronounced apoptosis than GAN. Collectively, the findings from 2 murine NASH models support the prevailing hypothesis in this study: overexpressed TrkB mitigated the initiation and progression of hepatic fibrosis through inhibiting the TGF-β/SMAD signaling pathway in NASH fibrotic progression.

DISCUSSION

In the present study, TrkB has been demonstrated to function as a negative regulator of hepatic fibrogenesis for the first time. The findings revealed that TrkB blocked TGF-β/SMAD signaling by suppressing the

phosphorylation and nuclear translocation of SMAD2/3, leading to the inhibition of HSC activation and proliferation. During the progression of hepatic fibrosis, TGF-β1–induced Ndfip1 promoted TrkB degradation through the ubiquitin-proteasome pathway, resulting in the activation of downstream fibrogenic genes. Moreover, the overexpression of TrkB in either HSCs or hepatocytes using AAV6/8 vectors attenuated liver fibrosis in mouse models.

It has been well documented that the inactivation of TGFBR1/2 or SMAD3 significantly repressed fibrosis progression in various models. Antibody-mediated inhibition of TGF-β downstream targets such as CTGF, IL-11, or c-Jun attenuated fibrosis in various models.[4] However, TGF-β is ubiquitously expressed, and no effective drugs designed for targeting the TGF-β signaling have been approved, mainly because of poor druggability or toxicity.[4,6] Herein, the present study endeavored to specifically express TrkB in HSCs as a new therapeutic strategy for fibrosis alleviation.

It has been proposed that the nervous system is associated with hepatic glucose and lipid metabolism,[25] emphasizing the importance of the brain-liver axis in organ-organ communication. Moreover, the reduced levels of arachidonic acid and docosahexaenoic acid in the brain were closely linked to hepatic fibrosis.[26] On the other hand, liver fibrosis patients were confirmed to behave impaired cognitive issues.[27] Thus, brain-liver relationships were considered to play a role in the progression of hepatic fibrosis.[28] TrkB is a receptor of BDNF, is mainly expressed in the brain, and acts as a central regulator of neuronal functions.[8] The findings in the present study attain supporting evidence for the participation of the brain-liver axis in chronic liver disease.

There are 2 isoforms of TrkB: the truncated isoform of TrkB (TrkB-T1) and full-length TrkB. TrkB-T1 is more abundant than full-length TrkB and represses TrkB signaling.[29] A recent study has demonstrated that TrkB-T1 was upregulated during AMLN-induced NASH and that BDNF protected mice from diet-induced NASH by suppressing TrkB-T1.[30] However, no direct *in vitro* or *in vivo* evidence has been proved to depict the function of TrkB or TrkB-T1 in hepatic fibrosis. The present study confirmed that the TrkB inhibited the TGF-β/SMAD signaling pathway by directly interacting with SMAD proteins, which is consistent with a previous report in tumor cells.[31] Therefore, it is clear that the function and molecular mechanism of TrkB in hepatic fibrosis are distinctly different from TrkB-T1.[30]

Previous studies reported that the reduction of TrkB facilitated obesity both in humans and mice, mainly because of elevated food intake.[13] A recent report demonstrated that the protein level of TrkB was downregulated in ApoE−/− atherosclerotic model and that TrkB knockdown resulted in increased lipid deposition, presenting the negative regulation of TrkB in lipid formation.[14] However, there was no difference in adipocyte sizes between control and AAV8-TrkB–injected mice observed in the present study (Figure 7E). Nevertheless, it was found that lipid sensor CD36 was remarkably decreased when TrkB was overexpressed in hepatocytes (Figure S13C, http://links.lww.com/HEP/D445). Thus, the protective effects of TrkB against lipotoxicity warrant further investigations.

In conclusion, the findings in the present study demonstrated that TrkB is a negative regulator of hepatic fibrogenesis and revealed a novel regulatory mechanism between TrkB and TGF-β/SMAD signaling pathway. Furthermore, these findings render solid evidence for TrkB to be utilized as a molecular target for the intervention of liver fibrosis.

AUTHOR CONTRIBUTIONS

Guangqi Song, Qunyan Yao, and Yu Song: provided the concept, designed the study and provided the conceptual framework for the study. Xizhong Shen and Jiefei Cheng: provided the concept and the financial support. Yu Song, Jiayi Wei, Rong Li, and Ruifeng Fu: performed all experiments and analyzed the data. Pei Han, Heming Wang, Guangcong Zhang, Shuyu Li, Sinuo Chen, and Zhiyong Liu: analyzed the data. Yu Song wrote the manuscript with the help of Guangqi Song and Qunyan Yao. Jian Wu: contributed to manuscript preparation and finalization. Hao Pei provided DNA Origami for 3D liver spheroids. Yicheng Zhao, Changfeng Zhu, Jimin Zhu, Ling Dong, and Shuncai Zhang provided conceptual evaluation of the project.

ACKNOWLEDGMENTS

The authors thank Dr. Hui Qian, Otsuka Shanghai Research Institute, for providing HEK-Blue TGF-β cells (InvivoGen, Cat. hkb-tgfb) and helpful comments on this manuscript. The authors also thank Zhen Yang for helping analyze transcriptome data.

FUNDING INFORMATION

This work was supported by China Postdoctoral Science Foundation (No. 2020M671010 to Yu Song), Horizontal Project with Otsuka of Joint Training Postdoctoral Program (No. H2020-016 to Xizhong Shen), Shanghai Science and Technology Committee (No. 22140900700 to Qunyan Yao), Natural Science Foundation of Shanghai (No. 20ZR1411200 to Guangqi Song), National Natural Science Foundation of China (No. 81700550 to Guangqi Song), and National Natural Science Foundation of China (No. 81871997 and 82170624 to Jian Wu).

CONFLICTS OF INTEREST

Jiefei Cheng and Pei Han are the employees of Otsuka Pharmaceutical Co., Ltd. Yicheng Zhao and Guangqi Song are the employees of Puheng Technology Co., Ltd. The remaining authors have no conflicts to report.

DATA AVAILABILITY STATEMENT

The authors declare that supporting data of this study are available within its supplementary information files. The transcriptome sequencing data generated in this study have been deposited in NCBI's Gene expression Omnibus and are accessible through GEO Series accession number PRJNA825841.

ORCID

Yu Song https://orcid.org/0000–0002–5749–0691
Jiayi Wei https://orcid.org/0009–0002–0922–5890
Rong Li https://orcid.org/0000–0001–8482–5701
Ruifeng Fu https://orcid.org/0009–0003–1603–1151
Pei Han https://orcid.org/0000–0003–0983–2471
Heming Wang https://orcid.org/0009–0003–9124–8238
Guangcong Zhang https://orcid.org/0000–0003–3105–1903
Shuyu Li https://orcid.org/0000–0001–9318–5849
Sinuo Chen https://orcid.org/0009–0006–9433–5400
Zhiyong Liu https://orcid.org/0000–0002–7135–2746
Yicheng Zhao https://orcid.org/0000–0002–1691–323X
Changfeng Zhu https://orcid.org/0000–0002–4922–0659
Jimin Zhu https://orcid.org/0000–0002–2150–473X
Shuncai Zhang https://orcid.org/0000–0003–2031–4595
Hao Pei https://orcid.org/0000–0002–6885–6708
Jiefei Cheng https://orcid.org/0000–0002–5902–0490
Jian Wu https://orcid.org/0000–0001–9933–7364
Ling Dong https://orcid.org/0000–0001–5995–7673
Guangqi Song https://orcid.org/0000–0002–2409–0771
Xizhong Shen https://orcid.org/0000–0003–3748–0709
Qunyan Yao https://orcid.org/0000–0003–3586–1911

REFERENCES

1. Aydın MM, Akçalı KC. Liver fibrosis. Turk J Gastroenterol. 2018; 29:14–21.
2. Sun M, Kisseleva T. Reversibility of liver fibrosis. Clin Res Hepatol Gastroenterol. 2015;39:S60–3.
3. Trautwein C, Friedman SL, Schuppan D, Pinzani M. Hepatic fibrosis: concept to treatment. J Hepatol. 2015;62:S15–24.
4. Budi EH, Schaub JR, Decaris M, Turner S, Derynck R. TGF-β as a driver of fibrosis: physiological roles and therapeutic opportunities. J Pathol. 2021;254:358–73.
5. Walton KL, Johnson KE, Harrison CA. Targeting TGF-β mediated SMAD signaling for the prevention of fibrosis. Front Pharmacol. 2017;8:461.
6. Györfi AH, Matei AE, Distler JHW. Targeting TGF-β signaling for the treatment of fibrosis. Matrix Biol. 2018;68-69:8–27.
7. Henderson NC, Rieder F, Wynn TA. Fibrosis: from mechanisms to medicines. Nature. 2020;587:555–66.
8. Skaper SD. The biology of neurotrophins, signalling pathways, and functional peptide mimetics of neurotrophins and their receptors. Cns Neurol Disord-Dr. 2008;7:46–62.
9. Tsai SJ. TrkB partial agonists: potential treatment strategy for major depression. Med Hypotheses. 2007;68:674–6.
10. Qin X, Zhao Y, Zhang T, Yin C, Qiao J, Guo W, Lu B. TrkB agonist antibody ameliorates fertility deficits in aged and cyclophosphamide-induced premature ovarian failure model mice. Nat Commun. 2022;13:914.
11. Hsiao SJ, Zehir A, Sireci AN, Aisner DL. Detection of tumor NTRK gene fusions to identify patients who may benefit from TRK inhibitor therapy. J Mol Diagn. 2019;21:553–71.
12. Gatalica Z, Xiu J, Swensen J, Vranic S. Molecular characterization of cancers with NTRK gene fusions. Modern Pathol. 2019;32:147–53.
13. Yeo GS, Connie Hung CC, Rochford J, Keogh J, Gray J, Sivaramakrishnan S, et al. A de novo mutation affecting human TrkB associated with severe obesity and developmental delay. Nat Neurosci. 2004;7:1187–9.
14. Jiang H, Huang S, Li X, Li X, Huang S, Zhang Y, et al. Endothelial tyrosine kinase receptor B prevents VE-cadherin cleavage and protects against atherosclerotic lesion development in ApoE-/- mice. Oncotarget. 2015;6:30640–9.
15. Ajmera V, Loomba R. Imaging biomarkers of NAFLD, NASH, and fibrosis. Mol Metab. 2021;50:101167.
16. MacParland SA, Liu JC, Ma XZ, Innes BT, Bartczak AM, Gage BK, et al. Single cell RNA sequencing of human liver reveals distinct intrahepatic macrophage populations. Nat Commun. 2018;9:4383.
17. Aoyama T, Inokuchi S, Brenner DA, Seki E. CX3CL1-CX3CR1 interaction prevents carbon tetrachloride-induced liver inflammation and fibrosis in mice. Hepatology. 2010;52:1390–400.
18. Schulien I, Hockenjos B, Schmitt-Graeff A, Perdekamp MG, Follo M, Thimme R, et al. The transcription factor c-Jun/AP-1 promotes liver fibrosis during non-alcoholic steatohepatitis by regulating osteopontin expression. Cell Death Differ. 2019;26:1688–99.
19. Xu B, Goulding EH, Zang K, Cepoi D, Cone RD, Jones KR, et al. Brain-derived neurotrophic factor regulates energy balance downstream of melanocortin-4 receptor. Nat Neurosci. 2003;6: 736–42.
20. Gupta VK, You Y, Gupta VB, Klistorner A, Graham SL. TrkB receptor signalling: implications in neurodegenerative, psychiatric and proliferative disorders. Int J Mol Sci. 2013;14:10122–42.
21. Jang SW, Liu X, Yepes M, Shepherd KR, Miller GW, Liu Y, et al. A selective TrkB agonist with potent neurotrophic activities by 7,8-dihydroxyflavone. Proc Natl Acad Sci USA. 2010;107: 2687–92.
22. Murray SS, Wong AW, Yang J, Li Y, Putz U, Tan SS, et al. Ubiquitin regulation of Trk receptor trafficking and degradation. Mol Neurobiol. 2019;56:1628–36.
23. Rezvani M, Espa.ol-Su.er R, Malato Y, Dumont L, Grimm Andrew A, Kienle E, et al. In vivo hepatic reprogramming of myofibroblasts with AAV vectors as a therapeutic strategy for liver fibrosis. Cell Stem Cell. 2016;18:809–16.
24. Pinheiro D, Dias I, Ribeiro Silva K, Stumbo AC, Thole A, Cortez E, et al. Mechanisms underlying cell therapy in liver fibrosis: an overview. Cells. 2019;8:1339.
25. Matsubara Y, Kiyohara H, Teratani T, Mikami Y, Kanai T. Organ and brain crosstalk: the liver-brain axis in gastrointestinal, liver, and pancreatic diseases. Neuropharmacology. 2022;1:108915.
26. Chen CC, Huang LT, Tain YL, Chaung HC, Hsieh CS, Eng HL, et al. Reduced brain content of arachidonic acid and docosahexaenoic acid is related to the severity of liver fibrosis. Digest Dis Sci. 2010;55:2831–7.
27. Weinstein G, Davis-Plourde K, Himali JJ, Zelber-Sagi S, Beiser AS, Seshadri S. Non-alcoholic fatty liver disease, liver fibrosis score and cognitive function in middle-aged adults: the Framingham Study. Liver Int. 2019;39:1713–21.
28. Bordet R, Deplanque D. Brain-liver axis: a new pathway for cognitive disorders related to hepatic fibrosis. Eur J Neurol. 2020;27:2111–2.

29. Fenner BM. Truncated TrkB: beyond a dominant negative receptor. Cytokine Growth F R. 2012;23:15–24.
30. Xiong J, Liu T, Mi L, Kuang H, Xiong X, Chen Z, et al. hnRNPU/TrkB defines a chromatin accessibility checkpoint for liver injury and non-alcoholic steatohepatitis pathogenesis. Hepatology. 2020;71:1228–46.
31. Kim MS, Jin W. TrkB-induced inhibition of R-SMAD/SMAD4 activation is essential for TGF-β-mediated tumor suppressor activity. Cancers. 2020;12:1048.

How to cite this article: Song Y, Wei J, Li R, Fu R, Han P, Wang H, et al. Tyrosine kinase receptor B (TrkB) attenuates liver fibrosis via inhibiting TGF-β/SMAD signaling. Hepatology. 2023;78:1433–1447. https://doi.org/10.1097/HEP.0000000000000319